

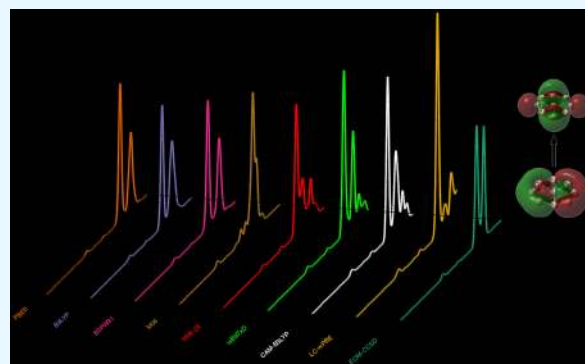
# Benchmarking Quantum Chemical Methods for Optical Absorption in Boron Wheels

Ravindra Shinde\*

Materials Research Center, Indian Institute of Science, Bangalore, Karnataka 560012, India

## Supporting Information

**ABSTRACT:** We benchmark various quantum chemical methods for calculating the optical absorption in planar boron wheel clusters. The geometries of neutral planar boron wheels  $B_7$ ,  $B_8$ , and  $B_9$  clusters are optimized at the coupled-cluster singles doubles level of theory. The optical absorption spectra of these clusters are calculated using three wave-function-based methods, namely, configuration interaction singles, random phase approximation, and equation-of-motion coupled-cluster singles doubles (EOM-CCSD) as well as using a time-dependent density-functional-theory-based method using various hybrid and long-range-corrected exchange and correlation functionals. There is an ample variation in the optical absorption spectra computed using different density functionals. When compared to the EOM-CCSD spectrum, an excellent agreement is provided by CAM-B3LYP functional, followed by  $\omega$ B97xD functional. PBE0, B3LYP, and B3PW91 functionals agree among each other. However, their spectra are red-shifted with respect to the EOM-CCSD counterpart. On the basis of the natural transition orbital analysis, the nature of optical excitation is also discussed.



## 1. INTRODUCTION

Clusters of atoms exhibit novel structures and properties, providing insights into new stoichiometries and chemical bondings. Planar boron clusters, in particular, have proven to be interesting because of the multiple aromaticities and extreme coordination environments.<sup>1–5</sup> Atoms of boron can adopt such an arrangement that they form a miniature wheel, with one atom at the center.  $B_{13}^+$  and  $B_{13}^-$  perform Wankel motor action when shined by circularly polarized light.<sup>6–8</sup> Such clusters have been synthesized, and their electronic structure is now well known.<sup>1</sup> Boron with seven, eight, and nine atoms forms such truly planar wheel structures with radii of 1.65, 1.80, and 2.0 Å, respectively. Although a lot of information about planarity, electronic structure, and chemical bonding is now available, the optical absorption of these clusters remains unexplored. Study of optical properties of such materials helps exploring applications in nanoplasmonics, photovoltaics, and so forth. Several methods exist for the calculation of optical absorption in these clusters. We present here benchmarking of various quantum chemical methods to get highly accurate results with relatively less computation.

To describe the ground state of a system, normally a reference state is used, which is a good approximation to the exact ground state of the system. Typically, variationally optimal solutions are recommended, although this is not the only possible way. This reference state cannot be a natural choice when it comes to electronic excited states. The variational collapse of optimization becomes preventive under

such circumstances. Coupled-cluster methods offer insensitivity to such single reference owing to the exponential treatment of single excitation effects.<sup>9</sup>

Equation-of-motion-coupled cluster is one of the approaches that can effectively and unambiguously describe the excited states of molecules or polyradicals where ground or excited states are often degenerate. Because it does not make any assumptions about the nature of the states, it is an easy-to-use single reference method. Also, it is the most accurate method in calculating one-electron vertical transition states. Often, the cluster expansion is terminated at doubles for computational feasibility, without serious compromise on the quality of results. The results can always be systematically improved by including more excitation levels. However, this method scales as  $N^6$ ,  $N$  being the number of basis functions, thereby making it intractable for large molecules.

We give here an account of other less expensive quantum chemical methods that can approximate the accurate equation-of-motion coupled-cluster singles doubles (EOM-CCSD) results. Only single-reference methods have been used to enable even nonspecialists for straightforward use with meaningful insights. In particular, the time-dependent density functional theory (TDDFT) with adiabatic approximation continues to remain favorite for the study of a large variety

Received: July 31, 2016

Accepted: October 3, 2016

Published: October 13, 2016

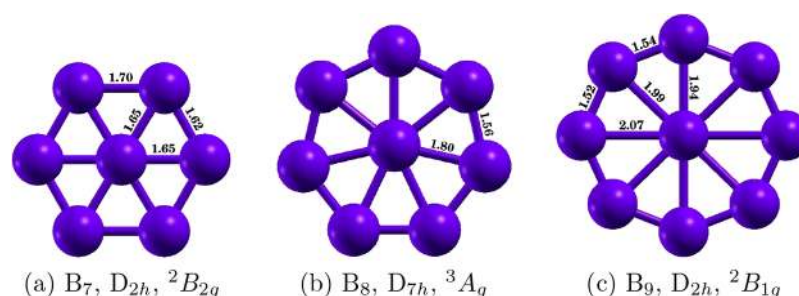


**Figure 1.** Geometry optimized structures of boron wheels (a)  $B_7$ , (b)  $B_8$ , and (c)  $B_9$  with point group symmetry and electronic ground state. All numbers are in angstrom units.

of systems. The exact exchange and correlation functionals required in this approach are not known; several approximations have been made in that respect. This adds to the puzzle to choose the right functional for a given type of calculation.<sup>10–13</sup> This work provides a qualitative and quantitative analysis of benchmarking results of various single reference quantum chemical methods including different functionals for TDDFT. This study helps in computationally identifying the least expensive method/functional that mimics more accurate EOM-CCSD results of optical absorption. This work was inspired by similar studies of comparison of oscillator strengths and electronic transition energies of different sets of small organic molecules.<sup>14,15</sup> Caricato, Trucks, Frisch, and Wiberg found that for vertical transition energies the best average performance is obtained with the B3P86 functional having a small amount of Hartree–Fock (HF) exchange.<sup>14</sup> Whereas for oscillator strengths, the CAM-B3LYP functional gave results close to the reference one.<sup>15</sup> Because clusters studied in the present work are planar inorganic molecules with open shells, it would be useful to benchmark the quantum chemical methods for their optical absorption. This study is based on a self-authored thesis chapter.<sup>16</sup>

The remainder of the paper is organized as follows. Next section discusses the theoretical and computational details of the calculations. Results are presented and discussed in the section **Results and Discussion**. Conclusions and future directions are presented in the section **Conclusions and Outlook**. Detailed information about wave functions of excited states contributing to various photoabsorption peaks is given in **Supporting Information**.

## 2. THEORETICAL AND COMPUTATIONAL DETAILS

**2.1. Geometry Optimization.** The geometries of the boron wheel clusters were optimized using the computer code GAUSSIAN 09<sup>17</sup> using a 6-311++G(2d,2p) basis set and using the size-consistent coupled-cluster singles doubles (CCSD) method. Raw geometries based on the density functional method were used to initiate the optimization as reported by Wang and co-workers.<sup>1</sup> The results of the optimization are in accordance with the available reports. These optimized geometries were further used in the calculations of optical absorption spectra. **Figure 1** shows the final optimized geometries of the clusters studied in this paper.

The optical absorption spectra of these optimized geometries of the clusters are then calculated using various quantum chemical methods such as configuration interaction singles (CIS), EOM-CCSD, and TDDFT using the computer code GAUSSIAN 09.<sup>17</sup> Various exchange and correlation functionals were used to compute the optical absorption spectra using the

TDDFT approach. An augmented, correlation consistent, polarized valence double zeta basis set was used for all methods mentioned above. This basis set is well suited for optical absorption calculations.<sup>18,19</sup>

**2.1.1. Excited-State Calculation Methods.** The excited-state energies of clusters are obtained using the simplest wavefunction-based ab initio CIS approach. In this method, different configurations are constructed by promoting an electron from an occupied orbital to a virtual orbital. Excited states of the system will have a linear combination of all such substituted configurations, with corresponding variational coefficients. For open-shell systems, we have used unrestricted HF formalism for constructing CIS configurations. The energies of the excited states will then be obtained by diagonalizing the Hamiltonian in this configurational space.<sup>17</sup> The dipole matrix elements are calculated using the ground-state and excited-state wave functions. This is subsequently used for calculating the optical absorption cross section assuming a Lorentzian lineshape, with some artificial finite linewidth.

Because the CIS method does not include electron correlation, as single excitation does not mix with HF reference, it is improved by including perturbative doubles correction. This is known as CIS(D). If it includes selective doubles excitation, then it gives rise to what is known as random phase approximation (RPA).

Coupled cluster method is known to include electron correlation in a systematic manner. Coupled cluster is an exact formalism if all possible excitations are taken into account. The excitation level is often terminated at doubles, which gives rise to the CCSD method. This method is extended to excited-state calculations through what is known as EOM-CCSD.<sup>20,21</sup> The computational time for this approach scales as  $N^6$ , where  $N$  is the number of basis functions, thereby limiting its use to smaller molecules.

**2.1.2. TDDFT Calculations.** Development of density functional theory (DFT) has led to an enormous progress in the understanding of properties of various systems. However, the main drawback is its dependence on the choice of exchange–correlation (XC) functional. Many different functionals are proposed for various kinds of calculations and the number is still counting. The time-dependent counterpart of DFT also uses the same functionals to investigate the excited-state properties. Here, we have considered various standard DFT XC functionals of various types to study the excited-state properties and optical absorption in boron clusters. The set of functionals includes (a) hybrid generalized-gradient approximation (H-GGA)—B3LYP,<sup>22–25</sup> B3PW91,<sup>22,26</sup> and PBE0,<sup>27–30</sup> (b) global hybrid-meta GGA (HM-GGA)—M06<sup>31</sup> and M06-2X,<sup>31</sup> and

(c) long-range corrected— $\omega$ B97xD,<sup>32</sup> CAM-B3LYP,<sup>33</sup> and LC- $\omega$ PBE.<sup>34–37</sup>

A local or semilocal density functional approximation to the XC functional often leads to a self-interaction error. Also, the XC potential has incorrect long-range behavior. In molecules, the XC potential of semilocal functionals decay exponentially as compared to the  $-1/\bar{r}$  form of exact asymptotic behavior of the XC potential.<sup>36</sup> Also, systems with an odd number of electrons, open-shell systems, or delocalized electrons are poorly described by local or semilocal density functional approximations. These issues can be resolved by mixing a certain amount of HF exchange into the DFT exchange and correlation functionals. With this resolution, the XC potential decays as  $-a/\bar{r}$  where  $a$  is the fraction of HF exchange mixture. Also, the exchange component of DFT can be split into two parts: (a) short range and (b) long range. A 100% HF exchange is used in the long-range limit to compensate part of the self-interaction error of DFT because HF exchange leads to an effective potential that has the correct asymptotic behavior.<sup>38</sup> Such a long-range-corrected class of functionals with an empirical separation parameter will be useful in describing molecules with delocalized electrons.<sup>34–36</sup>

The percentage of HF exchange in the XC functionals B3LYP, B3PW91, and PBE0 is 20%, 20%, and 25%, respectively. For Minnesota functionals M06 and M06-2X, HF exchange contributes 27% and 54%, respectively. The range-separated functionals have HF contribution depending upon the interelectronic distances. For example, in CAM-B3LYP, 19% HF exchange contributes in the short-range, whereas 65% HF exchange contributes in the long-range. The functional  $\omega$ B97xD with empirical dispersion has 22% and 100% exact exchange for short- and long-range, respectively. The performance of each of the above-mentioned functionals and other wave-function-based methods is discussed in the next section.

### 3. RESULTS AND DISCUSSION

In this section, we present vertical excitation energies for each cluster studied for different excited-state calculation methods, followed by the description of the photoabsorption spectra of boron wheel clusters studied. Graphical presentation of natural transition orbitals involved in TDDFT calculations is also given below.

**3.1. Vertical Excitation Energies.** Vertical excitation energies of first few excited states for each cluster are calculated. These values are reported separately in the Supporting Information. To get a comparative insight, we have taken the differences in vertical excitation energies of first four excited states for each method from the corresponding values of the EOM-CCSD reference. In the case of  $B_8$  cluster, the number of states considered is six because some of the states are degenerate. Figures 2–4 show the graphical presentation of these results for  $B_7$ ,  $B_8$ , and  $B_9$  clusters, respectively.

In the case of  $B_7$  cluster, the wave-function-based methods perform poorly because the deviation is too large from the reference. B3LYP, B3PW91, PBE0, and M06-2X provide red-shifted results compared to EOM-CCSD. A good compromise is made by CAM-B3LYP, M06, and  $\omega$ B97xD functionals because the deviation from reference is the least. PBE0 outperforms all other methods in the vertical energy calculations for the  $B_8$  cluster. CIS consistently overestimates the  $E_{ve}$  and so does RPA. Rest of the methods are within a

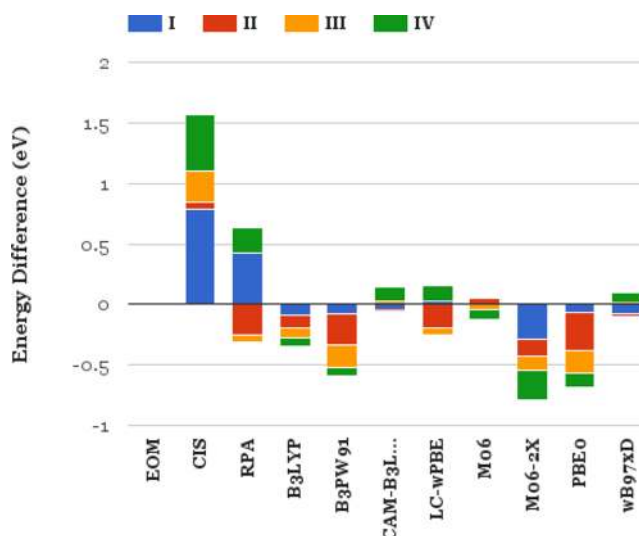


**Figure 2.** Vertical excitation energy differences  $\Delta E_{ve} = E_{ve_{QCM}} - E_{ve_{EOM}}$  for the first four excited states of the  $B_7$  cluster.

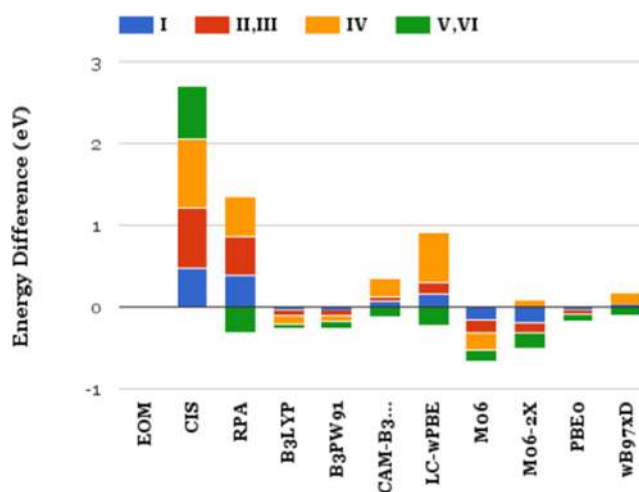


**Figure 3.** Vertical excitation energy differences  $\Delta E_{ve} = E_{ve_{QCM}} - E_{ve_{EOM}}$  for the first six excited states of the  $B_8$  cluster.

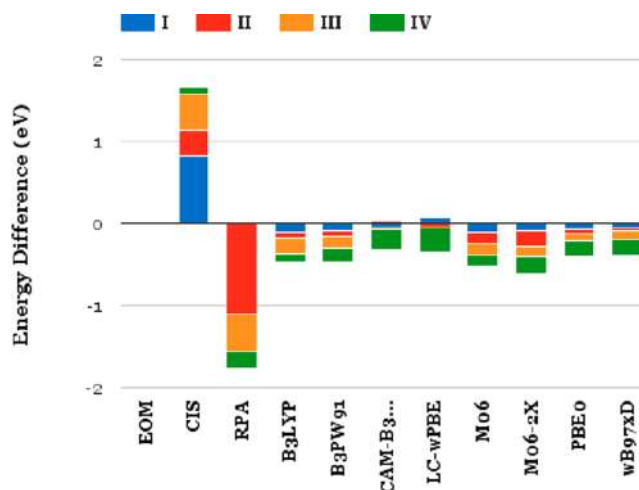


**Figure 4.** Vertical excitation energy differences  $\Delta E_{ve} = E_{ve_{QCM}} - E_{ve_{EOM}}$  for the first four excited states of the  $B_9$  cluster.

fraction of an eV from the reference EOM-CCSD calculations. CIS and RPA provide contrary results in the case of  $B_9$  clusters. All DFT functionals studied here provide roughly the same red-shifted deviation from the reference results in this case.

The comparison of absorption peak positions with the largest oscillator strengths obtained using various quantum chemical methods to the EOM-CCSD reference (see Table S4) is graphically shown in Figures 5 and 6. We have included cases of

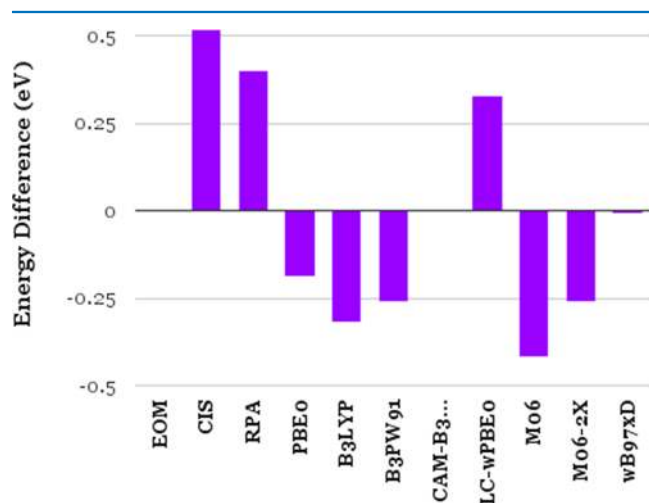


**Figure 5.** Difference in the peak energies corresponding to the largest oscillator strength  $\Delta E = E_{\text{QCM}} - E_{\text{EOM}}$  compared with the EOM-CCSD spectrum of  $B_8$ .

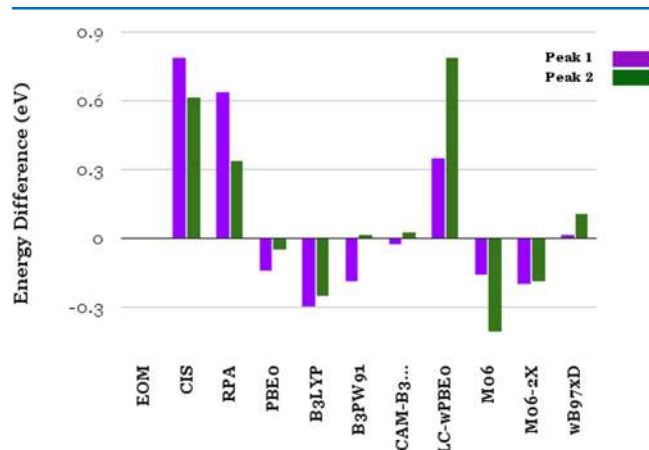


**Figure 6.** Difference in the peak energies corresponding to the largest oscillator strength  $\Delta E = E_{\text{QCM}} - E_{\text{EOM}}$  compared with the EOM-CCSD spectrum of  $B_9$ .

only  $B_8$  and  $B_9$  because their spectra contain well-defined intense peaks. In this study, a good performer will have  $\Delta E$  value as close to zero as possible. It is clearly seen that the wave-function-based methods largely overestimate the peak positions in the optical absorption spectra. On the other hand, CAM-B3LYP and  $\omega B97xD$  perform excellently on par with the reference EOM-CCSD calculations. Other hybrid-GGA functionals underestimate the energies of intense peaks in the absorption spectrum, whereas the long-range-corrected functional LC- $\omega$ PBE0 overestimates the energies.

**3.2. Calculated Photoabsorption Spectra of Various Clusters.** As evident in Figure 7, CIS largely overestimates the excitation energies in the optical absorption spectra of  $B_7$  as compared to the reference EOM-CCSD spectra. RPA shows

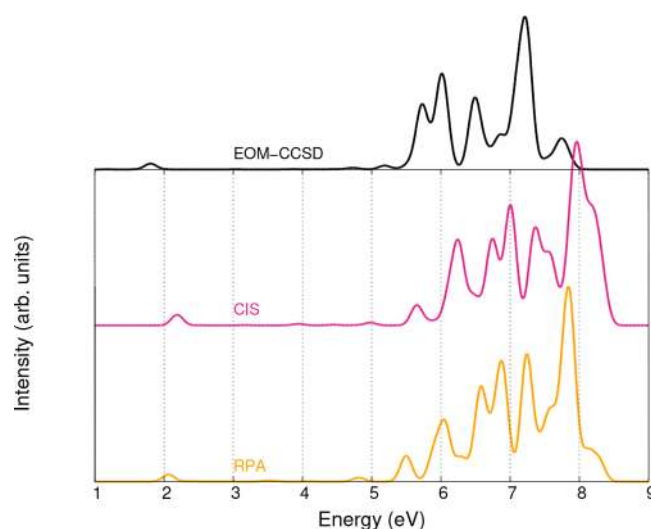


**Figure 7.** Linear optical absorption spectrum of the boron wheel  $B_7$  cluster calculated using EOM-CCSD, CIS, and RPA approaches. For plotting the spectrum, a uniform linewidth of 0.01 eV was used.

similar behavior but has smaller blue shifts as compared to CIS. Both CIS and RPA show higher intensities in all energy bands than the reference one. An excellent agreement is observed between EOM-CCSD and TDDFT results (see Figure 8) with

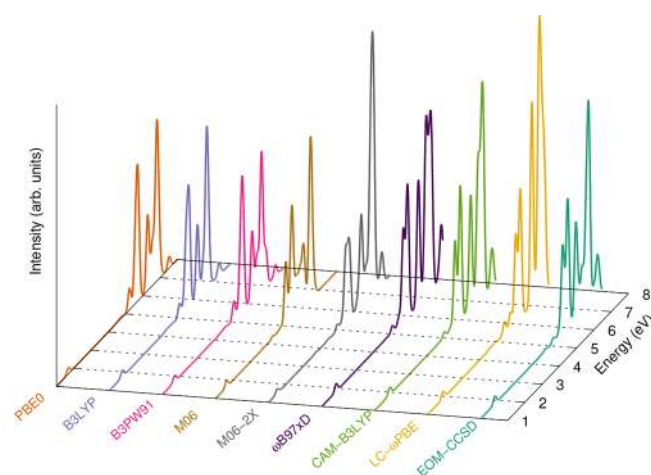


**Figure 8.** Linear optical absorption spectrum of the boron wheel  $B_7$  cluster calculated using the TDDFT approach using various functionals and compared to EOM-CCSD. For plotting the spectrum, a uniform linewidth of 0.01 eV was used.

$\omega B97xD$  and CAM-B3LYP functionals. This agreement holds good on the grounds of both excitation energies and oscillator strengths. However,  $\omega B97xD$  deviates from CAM-B3LYP spectra after 7 eV. M06 and M06-2X functionals show consistently red-shifted absorption throughout the spectrum. Other functionals, such as PBE0 and B3PW91, almost overlap each other in the low-energy regime. However, the former shifts toward blue from B3PW91 at higher energies. NTO analysis (see Figure 9) reveals that the nature of excitation for the peak at 1.63 eV is  $\pi \rightarrow \pi^*$ , and at 5.72 eV,  $\sigma \rightarrow \sigma^*$  dominates the excitation.

The optical absorption spectrum of  $B_8$  (Figures 10 and 11) shows very few and well-separated peaks. When compared with the EOM-CCSD spectrum, CIS and RPA show a large

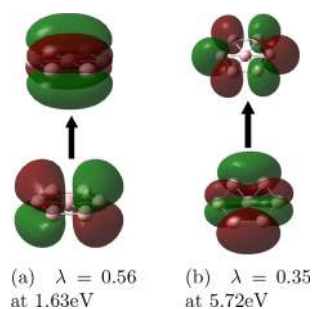


**Figure 9.** Natural transition orbitals (NTO) involved in the excited states of the  $B_7$  cluster calculated using the PBE0 method corresponding to the peak (a) at 1.63 eV with  $\lambda = 0.56$  ( $H_{\alpha} - 1 \rightarrow L_{\alpha}$ ) and to the peak (b) at 5.72 eV with  $\lambda = 0.35$  ( $H_{1\alpha} \rightarrow L_{\alpha} + 4$ ). The parameter  $\lambda$  refers to a fraction of the NTO pair contribution to a given electronic excitation.

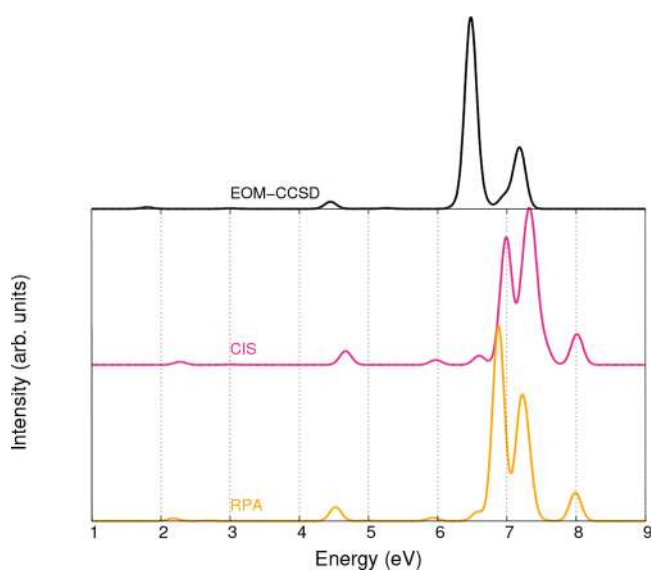


**Figure 10.** Linear optical absorption spectrum of the boron wheel  $B_8$  cluster calculated using CIS, EOM-CCSD, and RPA approaches. For plotting the spectrum, a uniform linewidth of 0.01 eV was used.

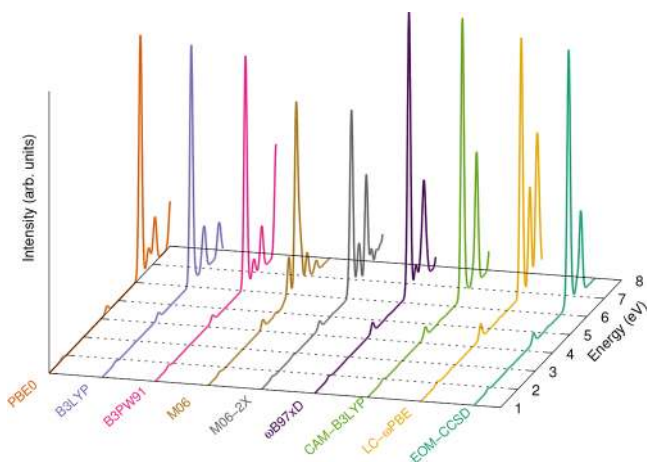


**Figure 11.** Linear optical absorption spectrum of the boron wheel  $B_8$  cluster calculated using the TDDFT approach using various functionals and compared to EOM-CCSD. For plotting the spectrum, a uniform linewidth of 0.01 eV was used.

overestimation of excitation energies. Again, CAM-B3LYP and  $\omega$ B97xD give an excellent agreement on the absorption spectrum when compared to the EOM-CCSD counterpart. At the strongest absorption peak, both energies and intensities of the spectra of these functionals match very well with each other in this case. M06 exhibits poor performance, with bands shifted to lower energies. Also, there are extra peaks observed at higher energies for this functional. M06-2X seems to correct the latter behavior while retaining the red shift of bands. PBE0, B3LYP, and B3PW91 spectra agree with each other at lower energies but start deviating afterward. The long-range-corrected functional LC- $\omega$ PBE has the same intensity profile as that of EOM-CCSD, but the peaks are generally blue-shifted by 0.2–0.4 eV. A pair of  $\sigma \rightarrow \pi^*$  transitions takes place at 1.77 eV, as seen from the NTO analysis in Figure 12.

The optical absorption spectrum of  $B_9$  also has very few intense peaks. Almost negligible absorption is seen at lower energies. As seen in Figure 13, the blue-shifted spectra of CIS and RPA show a large overestimation of the intensity. On the contrary, PBE0, B3LYP, B3PW91, M06, and M06-2X underestimate the position of the energy bands (see Figure 14). The spectrum of  $B_9$  is extremely overestimated by LC- $\omega$ PBE both in the position and in the intensities of bands. CAM-B3LYP and  $\omega$ B97xD again provide an excellent agreement on intensities and positions of energy bands. The peak at 1.71 eV is dominated by  $\sigma \rightarrow \sigma^*$ , and at 6.15 eV,  $\sigma \rightarrow \sigma^*$  transition takes place, as evident from the NTO analysis shown in Figure 15.

The CIS method, in general, overestimates the excitation energies because it does not include electron correlation effects. RPA with perturbative doubles slightly improves the excitation energies for all three clusters. This means that sophisticated electron-correlated methods, such as multireference configuration interaction method, can perform better because of systematic inclusion of electron correlation energies.<sup>18,19</sup> Hybrid-GGA functionals with the same amount of HF exchange contribution (i.e., B3PW91 and B3LYP) have almost overlapping optical absorption spectra and differ slightly compared with the PBE0 spectrum that has 25% HF exchange. This indicates that a self-interaction correction is necessary (in terms of inclusion of HF exchange). Minnesota functionals have a larger share of HF exchanges but their spectra are red-shifted. These functionals were originally optimized for thermochemistry and reaction kinetics; so, they may not perform well for electronic excitation calculations.<sup>38</sup> Range-corrected functionals perform better for optical absorption in planar boron wheel clusters as compared to the hybrid or metahybrid functionals because of extended nature of orbitals, where incorporation of HF exchange at different interelectronic distances helps in describing the correct asymptotic behavior. This is why spectra of CAM-B3LYP and  $\omega$ B97xD match very well with the EOM-CCSD spectrum. However, the spectrum of LC- $\omega$ PBE differs from the rest of the range-corrected functionals, especially at higher energies. This failure of the XC functional with the correct asymptotic behavior can be due to inaccurate transition dipoles between the valence states where only functionals with lower HF exchange perform well.<sup>39</sup>

The nature of optical excitation can be classified into molecular-type or collective/plasmonic-type depending upon the extent of mixing of configurations to many-body wave functions of excited states contributing to a particular peak. A strong mixing of configurations to the many-body wave functions of excited states suggests a collective or plasmonic excitation. On the other hand, a single dominant configuration

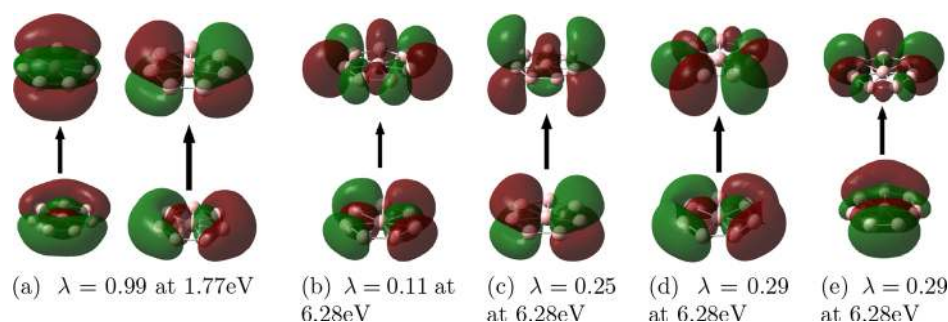


**Figure 12.** NTO involved in the excited states of the  $B_8$  cluster calculated using the PBE0 method corresponding to the peak (a) at 1.77 eV with  $\lambda = 0.99$  ( $H_\beta - 1 \rightarrow H_{1\beta}$  and  $H_\beta - 2 \rightarrow H_{2\beta}$ ) and to the peak at 6.28 eV (b) with  $\lambda = 0.11$  ( $H_\alpha - 2 \rightarrow L_\alpha + 3$ ), (c) 0.25 ( $H_\alpha - 1 \rightarrow L_\alpha + 2$ ), (d) 0.29 ( $H_\beta - 2 \rightarrow L_\beta + 1$ ), and (e) 0.29 ( $H_\beta - 1 \rightarrow L_\beta$ ). The parameter  $\lambda$  refers to a fraction of the NTO pair contribution to a given electronic excitation.

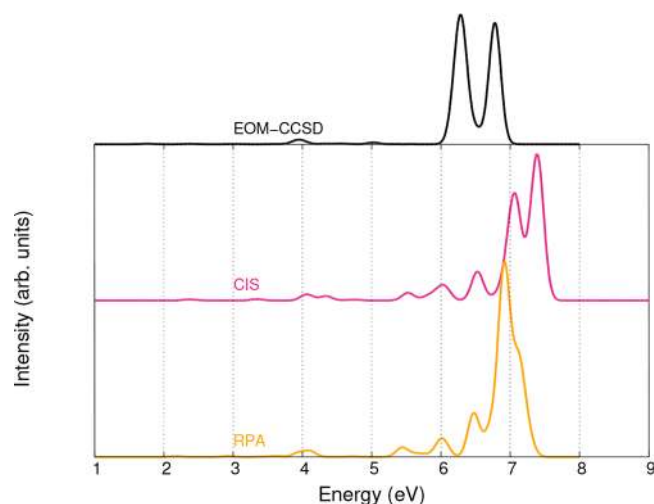


**Figure 13.** Linear optical absorption spectrum of the boron wheel  $B_9$  cluster calculated using CIS, EOM-CCSD, and RPA approaches. For plotting the spectrum, a uniform linewidth of 0.01 eV was used.

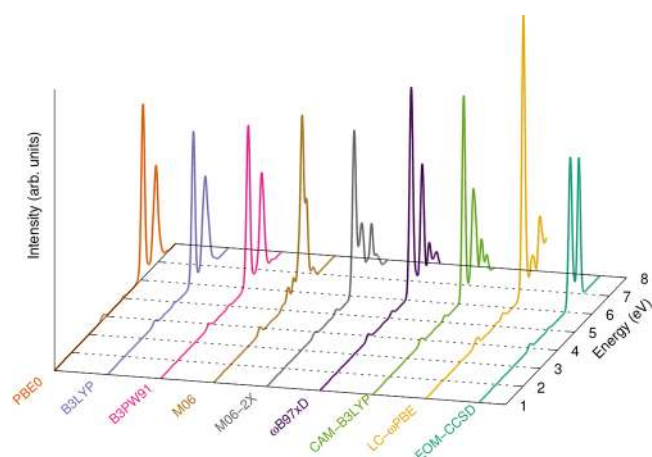


**Figure 14.** Linear optical absorption spectrum of the boron wheel  $B_9$  cluster calculated using the TDDFT approach using various functionals and compared to EOM-CCSD. For plotting the spectrum, a uniform linewidth of 0.01 eV was used.

contributing to the excited state suggests a molecular type of excitation.<sup>40,41</sup> The analysis of configurations contributing to EOM-CCSD many-body wave functions (see [Supporting Information](#)) of various excited states contributing to peaks of absorption spectra of these boron wheel clusters suggests that these excitations are of the collective plasmonic type. This

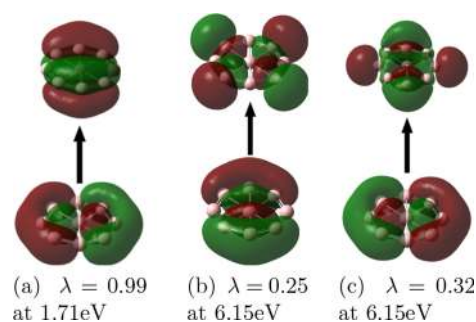


**Figure 15.** NTO involved in the excited states of the  $B_9$  cluster calculated using the PBE0 method corresponding to the peak (a) at 1.71 eV with  $\lambda = 0.99$  ( $H_\beta - 3 \rightarrow H_{1\beta}$ ), (b) at 6.15 eV with  $\lambda = 0.25$  ( $H_\beta - 3 \rightarrow L_\beta + 1$ ) and (c)  $\lambda = 0.32$  ( $H_\beta - 2 \rightarrow L_\beta$ ). The parameter  $\lambda$  refers to a fraction of the NTO pair contribution to a given electronic excitation.

fact is also confirmed in the NTO analysis of excited states, where several fractions ( $\lambda$ ) of the NTO pair contribution to a given electronic excitation have comparable weights.

#### 4. CONCLUSIONS AND OUTLOOK

The goal of the present study was to benchmark various single reference quantum chemical methods for calculating optical absorption spectra of planar boron wheel clusters. We sampled three wave-function-based methods and TDDFT with eight different XC functionals. Wave-function-based methods, such as RPA and CIS, consistently overestimate the excitation energies and oscillator strengths as compared to the EOM-CCSD calculations. The statistical analysis also reveals that the strongest peak positions are quite scattered from EOM reference values. To improve the situation, one should consider multireference methods because the test clusters have open-shell ground states.

Hybrid-GGA functionals—PBE0, B3LYP, and B3PW91—are also poor performers because they tend to underestimate the excitation energies. M06 and M06-2X are not indifferent in above-mentioned analysis. Among the long-range-corrected functionals, CAM-B3LYP provides the best agreement with EOM results both on the basis of oscillator strengths and excitation energies.

Although this study neither includes all functionals available nor are the test cases comprehensive, it helps in providing a reasonable comparison between various single reference methods and identifying the functionals that provide as good a result as EOM-CCSD in light of optical absorption

calculations. These findings can be tested against more sophisticated multireference calculations.<sup>18,19</sup>

## ■ ASSOCIATED CONTENT

### ● Supporting Information

The Supporting Information is available free of charge on the ACS Publications website at DOI: 10.1021/acsomega.6b00159.

Vertical excitation energies, excited-state wave functions, and oscillator strengths of boron wheel clusters (PDF)

## ■ AUTHOR INFORMATION

### Corresponding Author

\*E-mail: [ravindra@mrc.iisc.ernet.in](mailto:ravindra@mrc.iisc.ernet.in). Phone: +91-808-201-4793. Fax: +91-802-360-7316.

### Notes

The author declares no competing financial interest.

## ■ ACKNOWLEDGMENTS

The author (R.S.) thanks the Council of Scientific and Industrial Research (CSIR) and the Science and Engineering Research Board (SERB), Government of India, for research grants (09/087/(0600)2010-EMR-I) & (PDF/2015/000466). Fruitful discussions with Prof. Alok Shukla are kindly acknowledged.

## ■ REFERENCES

- (1) Zhai, H.-J.; Alexandrova, A. N.; Birch, K. A.; Boldyrev, A. I.; Wang, L.-S. Hepta- and Octacoordinate Boron in Molecular Wheels of Eight- and Nine-Atom Boron Clusters: Observation and Confirmation. *Angew. Chem., Int. Ed.* **2003**, *42*, 6004–6008.
- (2) Zhai, H.-J.; Kiran, B.; Li, J.; Wang, L.-S. Hydrocarbon Analogues of Boron Clusters—Planarity, Aromaticity and Antiaromaticity. *Nat. Mater.* **2003**, *2*, 827–833.
- (3) Alexandrova, A. N.; Boldyrev, A. I.; Zhai, H.-J.; Wang, L.-S. All-boron aromatic clusters as potential new inorganic ligands and building blocks in chemistry. *Coord. Chem. Rev.* **2006**, *250*, 2811–2866.
- (4) Alexandrova, A. N.; Zhai, H.-J.; Wang, L.-S.; Boldyrev, A. I. Molecular Wheel  $B_8^{2-}$  as a New Inorganic Ligand. Photoelectron Spectroscopy and ab Initio Characterization of  $LiB_8^-$ . *Inorg. Chem.* **2004**, *43*, 3552–3554.
- (5) Huang, W.; Sergeeva, A. P.; Zhai, H.-J.; Averkiev, B. B.; Wang, L.-S.; Boldyrev, A. I. A concentric planar doubly  $\pi$ -aromatic  $B_{19}^-$  cluster. *Nat. Chem.* **2010**, *2*, 202–206.
- (6) Jiménez-Halla, J. O. C.; Islas, R.; Heine, T.; Merino, G.  $B_{19}^-$ : An Aromatic Wankel Motor. *Angew. Chem., Int. Ed.* **2010**, *49*, 5668–5671.
- (7) Zhang, J.; Sergeeva, A. P.; Sparta, M.; Alexandrova, A. N.  $B_{13}^+$ : A Photodriven Molecular Wankel Engine. *Angew. Chem., Int. Ed.* **2012**, *51*, 8512–8515.
- (8) Merino, G.; Heine, T. And Yet It Rotates: The Starter for a Molecular Wankel Motor. *Angew. Chem., Int. Ed.* **2012**, *51*, 10226–10227.
- (9) Stanton, J. F.; Bartlett, R. J. The equation of motion coupled-cluster method. A systematic biorthogonal approach to molecular excitation energies, transition probabilities, and excited state properties. *J. Chem. Phys.* **1993**, *98*, 7029–7039.
- (10) Guo, H.-B.; He, F.; Gu, B.; Liang, L.; Smith, J. C. Time-Dependent Density Functional Theory Assessment of UV Absorption of Benzoic Acid Derivatives. *J. Phys. Chem. A* **2012**, *116*, 11870–11879.
- (11) Muniz-Miranda, F.; Pedone, A.; Battistelli, G.; Montalti, M.; Bloino, J.; Barone, V. Benchmarking TD-DFT against Vibrationally Resolved Absorption Spectra at Room Temperature: 7-Aminocoumarins as Test Cases. *J. Chem. Theory Comput.* **2015**, *11*, 5371–5384.

(12) Guidez, E. B.; Aikens, C. M. Origin and TDDFT Benchmarking of the Plasmon Resonance in Acenes. *J. Phys. Chem. C* **2013**, *117*, 21466–21475.

(13) Leang, S. S.; Zahariev, F.; Gordon, M. S. Benchmarking the performance of time-dependent density functional methods. *J. Chem. Phys.* **2012**, *136*, 104101–104112.

(14) Caricato, M.; Trucks, G. W.; Frisch, M. J.; Wiberg, K. B. Electronic Transition Energies: A Study of the Performance of a Large Range of Single Reference Density Functional and Wave Function Methods on Valence and Rydberg States Compared to Experiment. *J. Chem. Theory Comput.* **2010**, *6*, 370–383.

(15) Caricato, M.; Trucks, G. W.; Frisch, M. J.; Wiberg, K. B. Oscillator Strength: How Does TDDFT Compare to EOM-CCSD? *J. Chem. Theory Comput.* **2011**, *7*, 456–466.

(16) Shinde, R. Ab Initio Calculations of Optical Properties of Clusters. Ph.D. Thesis, Indian Institute of Technology, Bombay, 2014; arxiv:1607.06928.

(17) Frisch, M. J.; Trucks, G. W.; Schlegel, H. B.; Scuseria, G. E.; Robb, M. A.; Cheeseman, J. R.; Scalmani, G.; Barone, V.; Mennucci, B.; Petersson, G. A.; Nakatsuji, H.; Caricato, M.; Li, X.; Hratchian, H. P.; Izmaylov, A. F.; Bloino, J.; Zheng, G.; Sonnenberg, J. L.; Hada, M.; Ehara, M.; Toyota, K.; Fukuda, R.; Hasegawa, J.; Ishida, M.; Nakajima, T.; Honda, Y.; Kitao, O.; Nakai, H.; Vreven, T.; Montgomery, J. A., Jr.; Peralta, J. E.; Ogliaro, F.; Bearpark, M.; Heyd, J. J.; Brothers, E.; Kudin, K. N.; Staroverov, V. N.; Kobayashi, R.; Normand, J.; Raghavachari, K.; Rendell, A.; Burant, J. C.; Iyengar, S. S.; Tomasi, J.; Cossi, M.; Rega, N.; Millam, J. M.; Klene, M.; Knox, J. E.; Cross, J. B.; Bakken, V.; Adamo, C.; Jaramillo, J.; Gomperts, R.; Stratmann, R. E.; Yazyev, O.; Austin, A. J.; Cammi, R.; Pomelli, C.; Ochterski, J. W.; Martin, R. L.; Morokuma, K.; Zakrzewski, V. G.; Voth, G. A.; Salvador, P.; Dannenberg, J. J.; Dapprich, S.; Daniels, A. D.; Farkas, Ö.; Foresman, J. B.; Ortiz, J. V.; Cioslowski, J.; Fox, D. J. *Gaussian 09 Revision A.02*; Gaussian, Inc.: Wallingford, CT, 2009.

(18) Shinde, R.; Shukla, A. Large-scale first principles configuration interaction calculations of optical absorption in boron clusters. *Nano LIFE* **2012**, *2*, 1240004–1240024.

(19) Shinde, R.; Shukla, A. Large-scale first principles configuration interaction calculations of optical absorption in aluminum clusters. *Phys. Chem. Chem. Phys.* **2014**, *16*, 20714–20723.

(20) Kállay, M.; Gauss, J. Calculation of excited-state properties using general coupled-cluster and configuration-interaction models. *J. Chem. Phys.* **2004**, *121*, 9257–9269.

(21) Krylov, A. I. Equation-of-Motion Coupled-Cluster Methods for Open-Shell and Electronically Excited Species: The Hitchhiker's Guide to Fock Space. *Ann. Rev. Phys. Chem.* **2008**, *59*, 433–462.

(22) Becke, A. D. Density-functional exchange-energy approximation with correct asymptotic behavior. *Phys. Rev. A: At, Mol., Opt. Phys.* **1988**, *38*, 3098–3100.

(23) Lee, C.; Yang, W.; Parr, R. G. Development of the Colle-Salvetti correlation-energy formula into a functional of the electron density. *Phys. Rev. B: Condens. Matter Mater. Phys.* **1988**, *37*, 785–789.

(24) Miehlich, B.; Savin, A.; Stoll, H.; Preuss, H. Results obtained with the correlation energy density functionals of Becke and Lee, Yang and Parr. *Chem. Phys. Lett.* **1989**, *157*, 200–206.

(25) Becke, A. D. Density-functional thermochemistry. III. The role of exact exchange. *J. Chem. Phys.* **1993**, *98*, 5648–5652.

(26) Perdew, J. P. In *Electronic Structure of Solids*; Ziesche, P., Eschrig, H., Eds.; Akademie Verlag: Berlin, 1991.

(27) Perdew, J. P.; Burke, K.; Ernzerhof, M. Generalized Gradient Approximation Made Simple. *Phys. Rev. Lett.* **1996**, *77*, 3865–3868.

(28) Perdew, J. P.; Burke, K.; Ernzerhof, M. Generalized Gradient Approximation Made Simple. *Phys. Rev. Lett.* **1997**, *78*, 1396.

(29) Adamo, C.; Barone, V. Toward reliable density functional methods without adjustable parameters: The PBE0 model. *J. Chem. Phys.* **1999**, *110*, 6158–6170.

(30) Ernzerhof, M.; Scuseria, G. E. Assessment of the Perdew–Burke–Ernzerhof exchange–correlation functional. *J. Chem. Phys.* **1999**, *110*, 5029–5036.

- (31) Zhao, Y.; Truhlar, D. G. The M06 suite of density functionals for main group thermochemistry, thermochemical kinetics, non-covalent interactions, excited states, and transition elements: two new functionals and systematic testing of four M06-class functionals and 12 other function. *Theor. Chem. Acc.* **2007**, *120*, 215–241.
- (32) Chai, J.-D.; Head-Gordon, M. Long-range corrected hybrid density functionals with damped atom–atom dispersion corrections. *Phys. Chem. Chem. Phys.* **2008**, *10*, 6615–6620.
- (33) Yanai, T.; Tew, D. P.; Handy, N. C. A new hybrid exchange–correlation functional using the Coulomb-attenuating method (CAM-B3LYP). *Chem. Phys. Lett.* **2004**, *393*, 51–57.
- (34) Iikura, H.; Tsuneda, T.; Yanai, T.; Hirao, K. A long-range correction scheme for generalized-gradient-approximation exchange functionals. *J. Chem. Phys.* **2001**, *115*, 3540–3544.
- (35) Tawada, Y.; Tsuneda, T.; Yanagisawa, S.; Yanai, T.; Hirao, K. A long-range-corrected time-dependent density functional theory. *J. Chem. Phys.* **2004**, *120*, 8425–8433.
- (36) Vydrov, O. A.; Scuseria, G. E. Assessment of a long-range corrected hybrid functional. *J. Chem. Phys.* **2006**, *125*, 234109–234109.
- (37) Vydrov, O. A.; Heyd, J.; Krukau, A. V.; Scuseria, G. E. Importance of short-range versus long-range Hartree-Fock exchange for the performance of hybrid density functionals. *J. Chem. Phys.* **2006**, *125*, 074106–074106.
- (38) Peverati, R.; Truhlar, D. G. Quest for a universal density functional: the accuracy of density functionals across a broad spectrum of databases in chemistry and physics. *Philos. Trans. R. Soc., A* **2014**, *372*, 20120476.
- (39) Nayyar, I. H.; Masunov, A. E.; Tretiak, S. Comparison of TD-DFT Methods for the Calculation of Two-Photon Absorption Spectra of Oligophenylvinylenes. *J. Phys. Chem. C* **2013**, *117*, 18170–18189.
- (40) Blanc, J.; Bonačić-Koutecký, V. B.; Broyer, M.; Chevaleyre, J.; Dugourd, P.; Koutecký, J.; Scheuch, C.; Wolf, J. P.; Wöste, L. Evolution of the electronic structure of lithium clusters between four and eight atoms. *J. Chem. Phys.* **1992**, *96*, 1793–1809.
- (41) Bonačić-Koutecký, V.; Gaus, J.; Guest, M. F.; Koutecký, J. Ab initio configuration interaction study of excited states of LiNa<sub>3</sub> and Li<sub>2</sub>Na<sub>2</sub> clusters: Interpretation of absorption spectra. *J. Chem. Phys.* **1992**, *96*, 4934–4944.